

# An efficient electroporation protocol for the genetic modification of mammalian cells

Leonardo Chicaybam<sup>1,6\*</sup>, Camila Barcelos<sup>1\*</sup>, Barbara Peixoto<sup>1</sup>, Mayra Carneiro<sup>1</sup>, Cintia Gomez Limia<sup>1</sup>, Patrícia Redondo<sup>2,3</sup>, Carla Lira<sup>4,5</sup>, Flávio Paraguassú-Braga<sup>4</sup>, Zilton Vasconcelos<sup>5</sup>, Luciana Barros<sup>1</sup>, Martin Hernán Bonamino<sup>1,6</sup>

1- Programa de Carcinogênese Molecular, Coordenação de Pesquisa - Instituto Nacional de Câncer (INCA), Rio de Janeiro - Brazil

2- Instituto de Ciências Biomédicas, Universidade Federal do Rio de Janeiro, Rio de Janeiro, Brazil

3- Centro de Transplante de Medula Óssea, Instituto Nacional de Câncer, Rio de Janeiro, Brazil

4- Banco de Cordão Umbilical e Placentário, Instituto Nacional de Cancer (INCA), Rio de Janeiro – RJ

5- Instituto Fernandes Figueira, Fundação Oswaldo Cruz, Rio de Janeiro, Brazil

6- Fundação Instituto Oswaldo Cruz, Vice-presidência de Pesquisa e Laboratórios de Referência, Rio de Janeiro, Brazil.

\*LC and CB contributed equally to this work.

Leonardo Chicaybam: [leonardo.chicaybam@fiocruz.br](mailto:leonardo.chicaybam@fiocruz.br)

Camila Barcelos: [camilabarcelos2.cb@gmail.com](mailto:camilabarcelos2.cb@gmail.com)

Bárbara Peixoto: [baabicp@gmail.com](mailto:baabicp@gmail.com)

Mayra Carneiro: [mayra\\_dsc@hotmail.com](mailto:mayra_dsc@hotmail.com)

Cintia Gomez Limia: [cintiagomezlimia@yahoo.com](mailto:cintiagomezlimia@yahoo.com)

Patrícia Redondo: [predondo@inca.gov.br](mailto:predondo@inca.gov.br)

Carla Lira: [cplira2000@yahoo.com.br](mailto:cplira2000@yahoo.com.br)

Flávio Paraguassú-Braga: [fbraga@inca.gov.br](mailto:fbraga@inca.gov.br)

Zilton Vasconcelos: [zvasconcelos@gmail.com](mailto:zvasconcelos@gmail.com)

Luciana Barros: [lucianalpt@gmail.com](mailto:lucianalpt@gmail.com)

Martin Hernán Bonamino: [mbonamino@inca.gov.br](mailto:mbonamino@inca.gov.br)

Correspondence should be addressed to M.H.B:

Martin H Bonamino

Coordenação de Pesquisa

Rua André Cavalcanti, 37 – 6 andar

20231-050

Rio de Janeiro - RJ

[mbonamino@inca.gov.br](mailto:mbonamino@inca.gov.br)

50 **Abstract**

51

52 Genetic modification of cell lines and primary cells is an expensive and cumbersome  
53 approach, often involving the use of viral vectors. Electroporation using square wave  
54 generating devices, like Lonza's Nucleofector, is a widely used option, but the costs  
55 associated with the acquisition of electroporation kits and the transient transgene  
56 expression might hamper the utility of this methodology. In the present work we show  
57 that our in house developed buffers, termed Chicabuffers, can be efficiently used to  
58 electroporate cell lines and primary cells from murine and human origin. Using the  
59 Nucleofector II device, we electroporated 14 different cell lines and also primary cells,  
60 like mesenchymal stem cells and cord blood CD34+, providing optimized protocols for  
61 each of them. Moreover, when combined with Sleeping Beauty based transposon system,  
62 long-term transgene expression could be achieved in all types of cells tested. Transgene  
63 expression was stable and did not interfere with CD34+ differentiation to committed  
64 progenitors. We also show that these buffers can be used in CRISPR-mediated editing of  
65 *PDCDI* gene locus in 293T and human peripheral blood mononuclear cells. The  
66 optimized protocols reported in this study provide a suitable and cost-effective platform  
67 for the genetic modification of cells, facilitating the widespread adoption of this  
68 technology.

69

70

71

72

73

74

75

76

77

78

79

80

81

82

83

84

85

86

87

88

89

90

91

92

93

94

95

96

97

98 **Keywords: Electroporation, cell line, MSC, T lymphocyte, CD34, Transposon,**  
99 **CRISPR, PD-1, GFP, RNA**

## 100 Introduction

101

102

103

104

105

106

107

108

109

110

111

112

113

114

115

116

117

118

119

120

121

122

123

124

125

126

127

128

129

130

131

132

133

134

135

136

137

138

139

140

141

142

143

144

145

146

147

148

149

Cell lines are valuable tools for research development, constituting one of the pillars of experimental biology. Their unlimited proliferative capacity, high degree of homogeneity and relatively easy maintenance in culture allow the generation of large number of cells required for testing numerous candidate drugs (Barretina et al., 2012), -omics profiling (Blower et al., 2007; Griffin and Shockcor, 2004; Nishizuka et al., 2003) and signaling pathways studies (Park et al., 2010), to cite some examples. One of the areas that benefited the most with the use of cell lines was cancer research, with the derivation of several cell lines that can be used as models for different cancers. These cells are used to model disease in vitro and in vivo, providing information about oncogenesis related pathways and insights into therapeutic strategies (Gillet et al., 2013). Moreover, cell lines are central players in the biotechnology industry, being used in the production of biopharmaceuticals like antibodies, hormones, and bioactive proteins in general (Kuystermans and Al-Rubeai, 2015).

The use of cell lines in basic research is often associated with genetic modification protocols, which allow overexpression and/or silencing of desired genes in a controllable fashion. Recently, the development of gene editing tools like TALENs and CRISPRs provided a more precise control of gene insertion or deletion, extending the possible genomic manipulations (Kim and Kim, 2014). Methods to deliver foreign genetic material (DNA or RNA) usually rely in non-viral or viral vectors, with the former being preferred because of increased biosafety, easier production and faster translation. Electroporation is a non-viral method for gene transfer that is demonstrating encouraging results, being successfully used for the manufacture of antitumor lymphocytes (Ramanayake et al., 2015) and other applications (Kotnik et al., 2015), but the mechanism of DNA/RNA transfer is not fully understood (Satkauskas et al., 2012). Moreover, the use of electroporation is associated with extensive testing of electric parameters (pulse amplitude, volts) in order to optimize the protocol. Non-viral methods like liposomes and electroporation show varying efficiencies, with several cell lines and primary cells showing poor transfection rates and cell death (Wang et al., 2012; Yin et al., 2014). In the case of liposomes, the transfection of non-adherent cell lines is rather inefficient, showing good results only for some adherent cells (Behr, 2012; Jordan and Wurm, 2004).

Using a square wave pulse technology, Lonza's Nucleofector electroporator was shown to be very efficient in several cell lines and primary human and murine cells, inducing high expression of the transgene and substantial viability<sup>24</sup>. The pre-loaded electroporation programs suited for each cell line simplify the experimental setup, and the use of proprietary additives improves the transfection efficiency. However, the frequent use of Nucleofector electroporation kits implies in important costs for research labs, especially those in middle to low income countries. In a previous work, our group developed "in house" electroporation buffers (termed "Chicabuffers") that had comparable efficiency with Lonza's buffers for the transfection of the human T cell line Jurkat and primary T lymphocytes from mouse and human origin(Chicaybam et al., 2013). Electroporation strategies using Chicabuffers were recently successfully applied to colon cancer cell lines (de Souza et al., 2013) and human mesenchymal stem cells (MSC; unpublished data). In the present work we extend the efficiency analysis of Chicabuffers and the description of optimal electroporation conditions in a panel of cell lines and primary cells that represent relevant models for cell biology studies and disease comprehension. We selected 14 cell lines of mouse and human origin and primary human

150 cells (MSC, peripheral blood mononuclear cells -PBMCs - and cord blood CD34+ cells),  
151 showing that these buffers yield high transfection efficiencies and are a viable option for  
152 genetic modification using the Nucleofector IIB electroporator. For cells in which the  
153 levels of transgene expression was low, we developed SB-based transposon plasmids  
154 engineered to confer drug resistance, allowing fast and efficient drug based selection of  
155 cells representing fractions of the cell culture.

156

157 We selected cells lines representing models for hematopoietic neoplasias (HEL,  
158 K562, P815, Nalm-6 and Jurkat cell lines) and different solid tumor derived cell lines (A-  
159 549, B16-F10, HeLa, MCF-7, MDA-MB-231). Some of the tested cells represent  
160 classical cellular models for ectopic gene expression (293T, NIH-3T3), cell signaling  
161 (Jurkat and 293T), growth factor dependence (BA/F-3) or simply relevant cells in terms  
162 of therapy and cell differentiation (MSCs, PBMCs and Cord Blood CD34+ cells). In  
163 addition, we show that the level of transfection achieved using Chicabuffers allows  
164 efficient genomic edition of the potentially clinical relevant PD1 locus in human cells  
165 such as 293T and peripheral blood mononuclear cells (PBMCs) using the recently  
166 described CRISPR/Cas9 system (Jinek et al., 2012).

167

## 168 **Materials and Methods**

169

### 170 Ethics approval

171

172 The use of PBMCs and CD34+ cells from healthy donors was approved by an IRB  
173 (Brazilian National Cancer Institute - INCA - Ethics Committee – protocol 153/13) and  
174 donors signed review board approved informed consents. MSCs were obtained from  
175 healthy donors submitted to surgery for hernia repair at the Clementino Fraga Filho  
176 University Hospital. The patients provided written informed consent and the study was  
177 approved by the Hospital Research Ethics Committee.

178

### 179 Plasmids and Cloning

180

181 The pT3-GFP plasmid (Peng et al., 2009) was kindly provided by Dr. Richard  
182 Morgan (Surgery Branch - NCI). The pT2-GFP and SB100X (Mátés et al., 2009)  
183 constructs were kindly provided by Dr. Sang Wang Han (UNIFESP, Brazil). For the  
184 creation of pT3-Neo-EF1a-GFP plasmid, GFP was excised from pT3-GFP by digestion  
185 with AgeI/NotI and the neomycin resistance gene (NEO), which was synthesized by  
186 Genscript (Piscataway, NJ, USA), was inserted. The EF1a-GFP cassette was isolated  
187 from the plasmid pRRLsin.PPTs.EF1a.GFPpre (Bonamino et al., 2004) (provided by Dr.  
188 Didier Trono, EPFL, Switzerland) after digestion with ClaI/BstBI and inserted in pT3-  
189 NEO previously digested with ClaI. For CRISPR experiments, the plasmid encoding *S.*  
190 *pyogenes* Cas9 (WT) and a U6 promoter for guide RNA (gRNA) expression was acquired  
191 from Addgene (pX330; #42230). gRNA (5' CACCGGCCATCTCCCTGGCCCCCA 3')  
192 for Programmed Cell Death 1 (*PDCD-1*) was designed by Optimized CRISPR Design  
193 tool (<http://crispr.mit.edu/>) and cloned in pX330 (Addgene) using BbsI restriction site.  
194 pRGS-CR (Kim et al., 2011) was provided by Dr Amilcar Tanuri (Federal University of  
195 Rio de Janeiro, Brazil), and *PDCD1* target sequence cloned in EcoRI / BamHI sites,  
196 between a red fluorescent protein (RFP) and a GFP, resulting in an out-of-frame GFP.  
197 The GFP expression can be restored by CRISPR-mediated non-homologous end joining  
198 (NHEJ) repair. All plasmids were isolated using Qiamp Maxi prep kit from Qiagen

199 (Germany) and quantified using a Nanodrop spectrophotometer. The new constructs  
200 described in this report are available at Addgene.

201

202 Cell lines and primary cells

203

204 The origin and cell culture conditions for each cell line are described in Table S1.

205 The use of PBMCs from healthy donors was approved by an IRB (Brazilian National  
206 Cancer Institute - INCA - Ethics Committee) and donors signed review board approved  
207 informed consents. Within 24h after blood collection, leukocytes were harvested by  
208 filtration and washed with Phosphate Buffered Saline (PBS). A density gradient  
209 centrifugation using Ficoll-Hypaque®-1077 was performed. Cells were centrifuged for  
210 20min at 890g (slow acceleration/deceleration off), washed three times with PBS and  
211 used for nucleofection. For CD34+ cells separation, mononuclear cells (MNCs) were  
212 isolated from umbilical cord blood after Ficoll density gradient using the same protocol  
213 above described. CD34+ cells were isolated from MNCs using CD34 MicroBead Kit  
214 (Miltenyi Biotech) following the manufacturer's instructions. The utilization of CD34+  
215 cells was also approved by INCA's Ethics Committee.

216

217 MSCs were isolated from abdominal subcutaneous adipose tissue fragments  
218 obtained from healthy donors submitted to surgery for hernia repair at the Clementino  
219 Fraga Filho University Hospital. The patients provided written informed consent and the  
220 study was approved by the Hospital Research Ethics Committee. Fragments were cut into  
221 small pieces and incubated with 1 mg/ml collagenase type II (Sigma-Aldrich, MO, USA)  
222 under permanent shaking at 37°C for 30 minutes. The cell suspension was centrifuged at  
223 400 g, room temperature, for 10 minutes and the pellet was resuspended on PBS,  
224 followed by filtration with 100 µm mesh strainers. Cells were plated to expand MSCs at  
225 3×10<sup>4</sup> cells/cm<sup>2</sup> density with low-glucose Dulbecco's modified Eagle's medium (DMEM  
226 Low-glucose, Gibco, CA, USA) supplemented with 10% fetal bovine serum (Gibco, CA,  
227 USA) and 100 U/ml penicillin and 100 µg/ml streptomycin (Sigma-Aldrich, MO, USA).  
228 Cells were electroporated at passage 3.

229

230 Electroporation

231

232 Generic cuvettes were used for all the electroporations (Mirus Biotech®, Madison,  
233 WI, USA cat.: MIR 50121). Cells were resuspended in 100ul of the desired buffer and  
234 4ug of the reporter plasmid (pT2-GFP transposon) were added. For long term  
235 experiments, 1ug of SB100X was added. The seven different buffers tested in this work  
236 are described in Table S2. Cells were transferred to a sterile 0.2cm cuvette and  
237 electroporated using the reported program (table 1) of Lonza® Nucleofector® II  
238 electroporation system. After transfection, cells were gently resuspended in 1mL of pre-  
239 warmed RPMI medium supplemented only with 2mM L-Glutamine and 20% FCS. All  
240 cells were seeded in 12-well plates and grown at 37°C and 5% CO<sub>2</sub>. The medium was  
241 replaced by complete RPMI medium the following day and cells were maintained as  
242 described previously.

243

244 Electroporation Score determination

245

246 For non-adherent cell lines, viability determination was based on trypan blue  
247 exclusion and/or determination of the % of cells displaying viable cell FSC vs SSC  
248 parameters by flow cytometry analysis on cells negative after 7AAD staining. For

249 adherent cells, viability determination was calculated based on the % of the OD obtained  
250 in Crystal Violet staining assays at d+1 or d+3. Calculation was based on the formula %=  
251 100x [OD for control (non electroporated) cell line/(OD for control (non electroporated)  
252 cell line + OD for electroporated cell line). The "electroporation score" was calculated  
253 based on cell viability (after normalization against the viability of non-transfected cells)  
254 and transgene expression on d+1, and the score set to the formula "Viability  
255 (%)\*Expression (%)/F". A division factor (F=50 for adherent cell lines and F=100 for  
256 non-adherent cell lines) was used in the score formula to fit the results in the graph scale.

257

258 Crystal Violet staining

259

260 To assess viability of adherent cell lines, cells were plated in triplicate in 96-well  
261 microtiter plates immediately after electroporation. Cell viability was evaluated after 24  
262 hours and cell expansion was analyzed at day+1 by crystal violet. The crystal violet  
263 incorporation assay was performed by fixing the cells with ethanol for 10 min, followed  
264 by staining them with 0.05% crystal violet in 20% ethanol for 10 min and solubilization  
265 with methanol as reported (Faget et al., 2012). The plate was read on a spectrophotometer  
266 at 595 nm (SpectraMax 190, Molecular Devices, Sunnyvale, CA).

267

268 In vivo B16-F10 tumor model

269

270 B16F10 cells were electroporated with 4 $\mu$ g of pT3-NEO-EF1a-GFP and 1 $\mu$ g of  
271 SB100x in buffer 1S, program P-020 of Lonza Nucleofactor II. As negative controls, we  
272 electroporated cells only with pT3-NEO-EF1a-GFP. Each condition was plated in a 6-  
273 well plate. After reaching 80% confluence, G418 (Life Technologies) antibiotic was  
274 added at 2,000 $\mu$ g/mL. The medium was changed every three days and the antibiotic  
275 added. After selection with antibiotic or not, we injected 5x10<sup>5</sup> cells in the left flank of  
276 C57BL/6 mice. After 15 days, we excised the tumor and plated the cells in 25cm<sup>2</sup> culture  
277 flasks. After 24 hours, the culture medium was changed to eliminate non-adherent cells.  
278 After 3 days, the cells were recovered and analyzed by flow cytometry for GFP  
279 expression.

280

281 CD34+ differentiation assay

282

283 Electroporated CD34+ cells were assayed in two different concentrations, 5x10<sup>2</sup>  
284 and 2x10<sup>3</sup> cells/well. The cells were concentrated in 300 $\mu$ L and then added in 1.1x  
285 concentrated 3 mL Methocult™ H4034 (Stem Cell Technologies Inc., Vancouver,  
286 Canada) then seeded 2 wells of a six-well plates, 1.1mL/well. Cells were cultivated for  
287 three weeks at 37 °C in a humidified atmosphere supplemented 5% CO<sub>2</sub> in incubator  
288 300/3000 Series (Revco, Ohio, EUA). The colonies were identified and quantified using  
289 STEMvision™ (Stem Cell Technologies Inc.) for the burst-forming units-erythroid  
290 (BFU-E), colony-forming units-erythroid (CFU-E), colony-forming units-granulocyte or  
291 macrophage or granulocyte-macrophage (CFU-G/M/GM) and colony-forming units-  
292 granulocyte/erythroid/megakaryocyte/macrophage (CFU-GEMM).

293

294 Flow cytometry

295

296 FACSCalibur® (BD Bioscience) was used to perform morphologic evaluation of  
297 viability (FSC vs SSC) and GFP expression analysis. Cells were harvested the following  
298 days after transfection and resuspended in PBS at a concentration of 105 cells/500 $\mu$ L.

299 7AAD staining (eBioscience cat. 00-6693) was performed immediately before FACS  
300 acquisition following manufacturer instructions. Data were analyzed using the FlowJo  
301 software (Tree Star). The hematopoietic progenitor CD34<sup>+</sup> cells were evaluated for purity  
302 by staining with anti-CD34-PE (clone 581, BD Biosciences).

303

304 CRISPR-mediated gene editing

305

306 HEK293FT and PBMCs were electroporated with pX330-PDCD-1 (10 $\mu$ g) and  
307 pRGS-CR-target (5 $\mu$ g). Gene editions were evaluated by GFP<sup>+</sup>/RFP<sup>+</sup> ratio after 24 hours  
308 by flow cytometry. To characterize indels at *PDCD1* locus, genomic DNA of gene edited  
309 cells was isolated by phenol-chloroform. Amplification of the target region was  
310 performed by PCR using the forward 5'-CCCCAGCAGAGACTTCTCAA and the  
311 reverse 5'-AGGACCGGCTCAGCTCAC primers. The PCR fragment was ligated in  
312 pCR2.1 vector (TA Cloning<sup>®</sup> Kit, Life Technologies), transformed in DH5 $\alpha$  cells and  
313 single bacteria colonies has the plasmid DNA extracted and sequenced using the primers  
314 described above.

315

316 Short RNA and plasmid co-electroporation

317

318 After Ficoll gradient purification, PBMCs (107 cells) were electroporated with  
319 pRGS-CR-target (10 $\mu$ g) and 10-50pmol of FITC labeled RNA (Invitrogen) in  
320 Chicabuffer 3P and U-014 Nucleofector IIb program. Cells were left resting in  
321 RPMI+10%FCS for 24h at 37°C and 5% CO<sub>2</sub> and then evaluated by flow cytometry  
322 using ACCURI C6 (BD Bioscience).

323

324 Statistical analysis

325

326 Data from electroporation experiments were analyzed by one-way ANOVA  
327 followed by Tukey's multiple comparison test using GraphPad Prism 6 software.

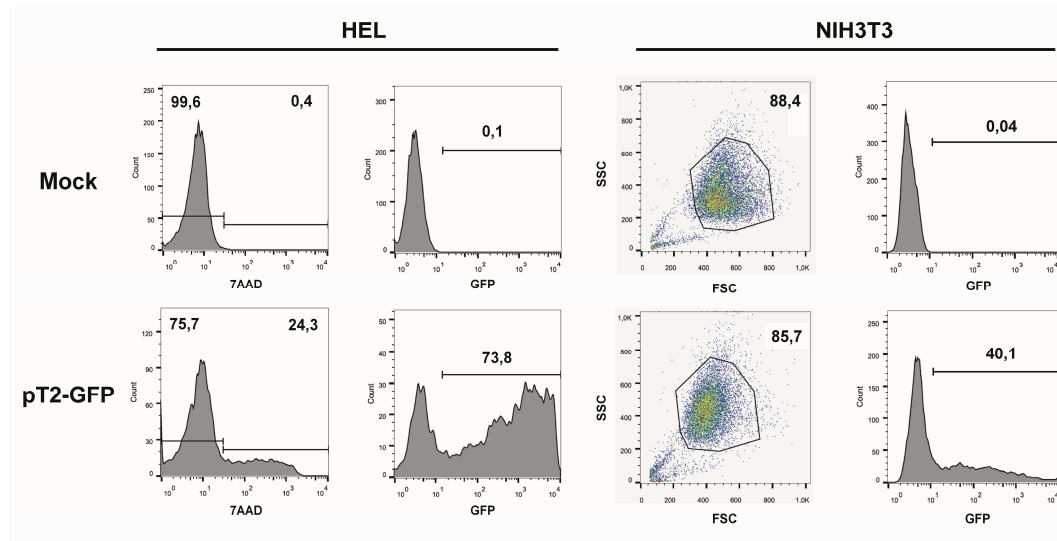
328

## 329 Results

330

331 With the objective of determining the best-suited buffer for the electroporation of  
332 each cell line, cells were electroporated with seven different buffers and the viability and  
333 GFP expression were analyzed. Representative flow cytometry plots are depicted in  
334 figure 1, showing 7AAD staining and GFP signal (gated in 7AAD negative cells) for a  
335 high electroporation score cell line (HEL) and FSC/SSC and GFP signal for a low score  
336 cell line (NIH3T3). 7AAD staining was performed only in the non-adherent cells since  
337 they represent a mixture of viable and non-viable cells at day 1 post electroporation.  
338 Adherent cells were allowed to adhere overnight after electroporation and non-  
339 adherent/dead cells were discarded before FACS analysis. As showed in figure 2, the  
340 majority of cell lines showed high electroporation scores independent of the buffer, with  
341 exception of P815, which showed an overall low efficiency but demonstrated best  
342 performance with buffer 3P. Suspension cell lines showed the best results regarding GFP  
343 expression, in which values above 60% were recurrently obtained. One exception is  
344 Nalm-6, with a maximum of 40% of GFP-positive cells obtained using buffer 3P.  
345 Adherent cell lines showed GFP values slightly lower (30-65%), with Hela showing the  
346 best result with 66,4 $\pm$ 8,3% of GFP expression using buffer 3P. Importantly, after 24h of  
347 electroporation the cells showed a good viability (Fig. 2), allowing expansion and  
348 recovery from the nucleofection. Viability and GFP expression were followed for 10 days

349 (suspension cell lines) or 7 days (adherent cell lines), with some cells retaining high levels  
350 of GFP (K562, HEL, B16) and others showing low expression of the marker after the  
351 expansion (NIH3T3, Jurkat, P815) (Figure S1-14). These results probably reflect the  
352 observed differences in nucleofection efficiency and proliferation rates among the studied  
353 cells. The electroporation protocol for each cell line is summarized in Table 1.  
354



355

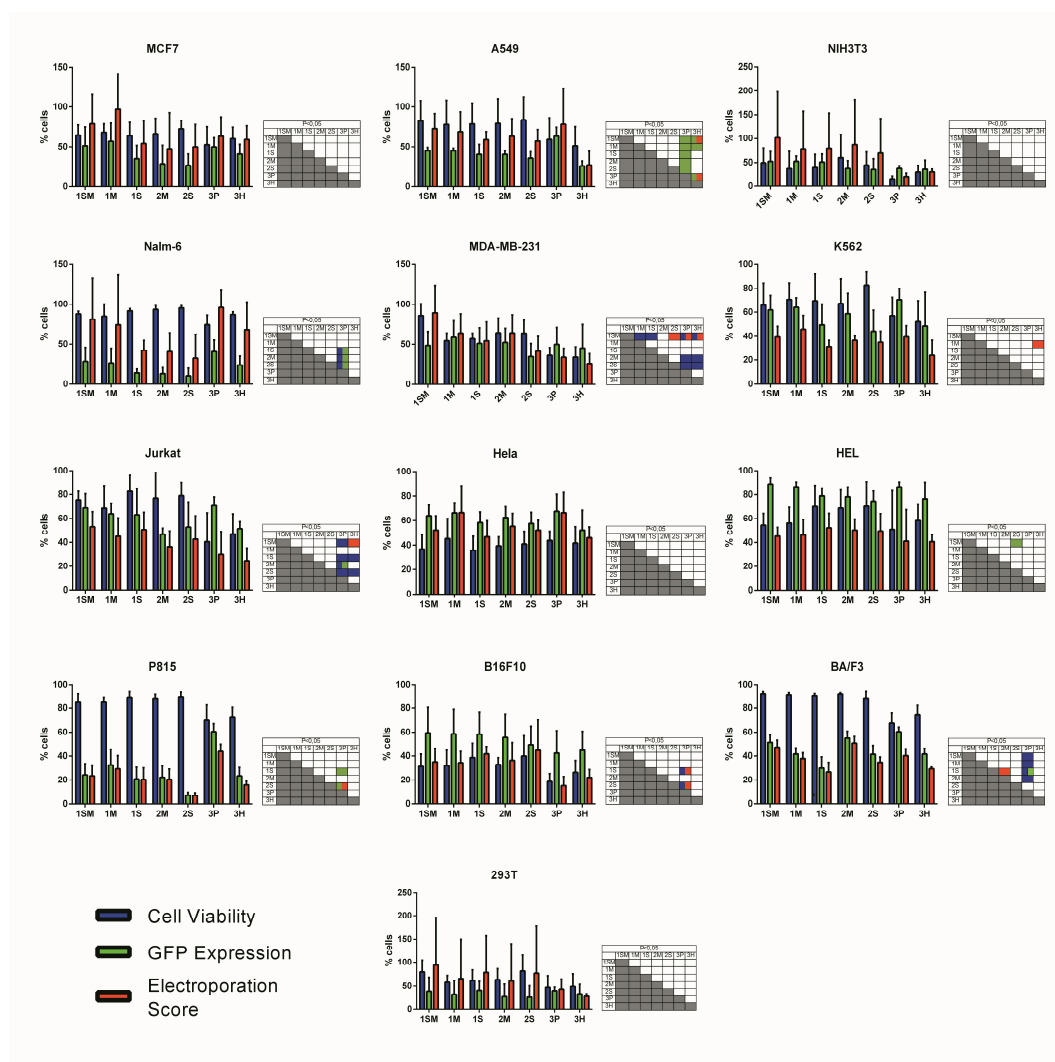
356 **Figure 1: GFP expression after electroporation of representative cell lines.**  
357 Representative plots of a high score cell line (HEL) and a low score cell line (NIH3T3).  
358 HEL was electroporated using buffer 2S and program X-005 and NIH3T3 using buffer  
359 1SM and program U-030. For HEL, on day one after nucleofection cells were stained  
360 with 7AAD (left column of graphs) and GFP expression was analyzed on 7AAD negative  
361 population (right column). For NIH3T3, viable cells were gated based in FSC/SSC and  
362 GFP was analyzed. Numbers depict the percentages of cells in each gate.

363

364 Stable gene expression is often required in the experimental setting, allowing the  
365 generation of subclones with overexpression or silencing of a gene of interest. The  
366 emergence of nonviral vectors that allow the integration of transgenes, like the Sleeping  
367 Beauty (SB) transposon system, simplified the genetic modification of cells, requiring  
368 only the delivery of two plasmids to achieve stable expression (one encoding the  
369 transgene flanked by ITRs – inverted terminal repeats – and one encoding the  
370 transposase). In order to evaluate if Chicabuffers could be used with this system, 1 $\mu$ g of  
371 SB100x (encoding a hyperactive version of the SB transposase) was electroporated with  
372 4 $\mu$ g of pT2-GFP and GFP expression was followed for 30 days. As showed in figure 3,  
373 the addition of the SB100x induced a higher percentage of GFP-positive cells after 30  
374 days of culture when compared with control cells, strongly suggesting that integration of  
375 the transgene has occurred. This effect was more pronounced in B16F10, HeLa and  
376 MCF7 cell lines, with approximately 20% of GFP-positive cells at day 30. The other cell  
377 lines showed only a modest increase in GFP-positive cells at day 30, ranging from 2%  
378 (BA/F-3) to 12% (K562). The long-term levels of GFP expression did not correlate with  
379 GFP expression at early days after nucleofection, suggesting that the cell lines have  
380 different intrinsic susceptibilities to SB-induced transgene integration.  
381

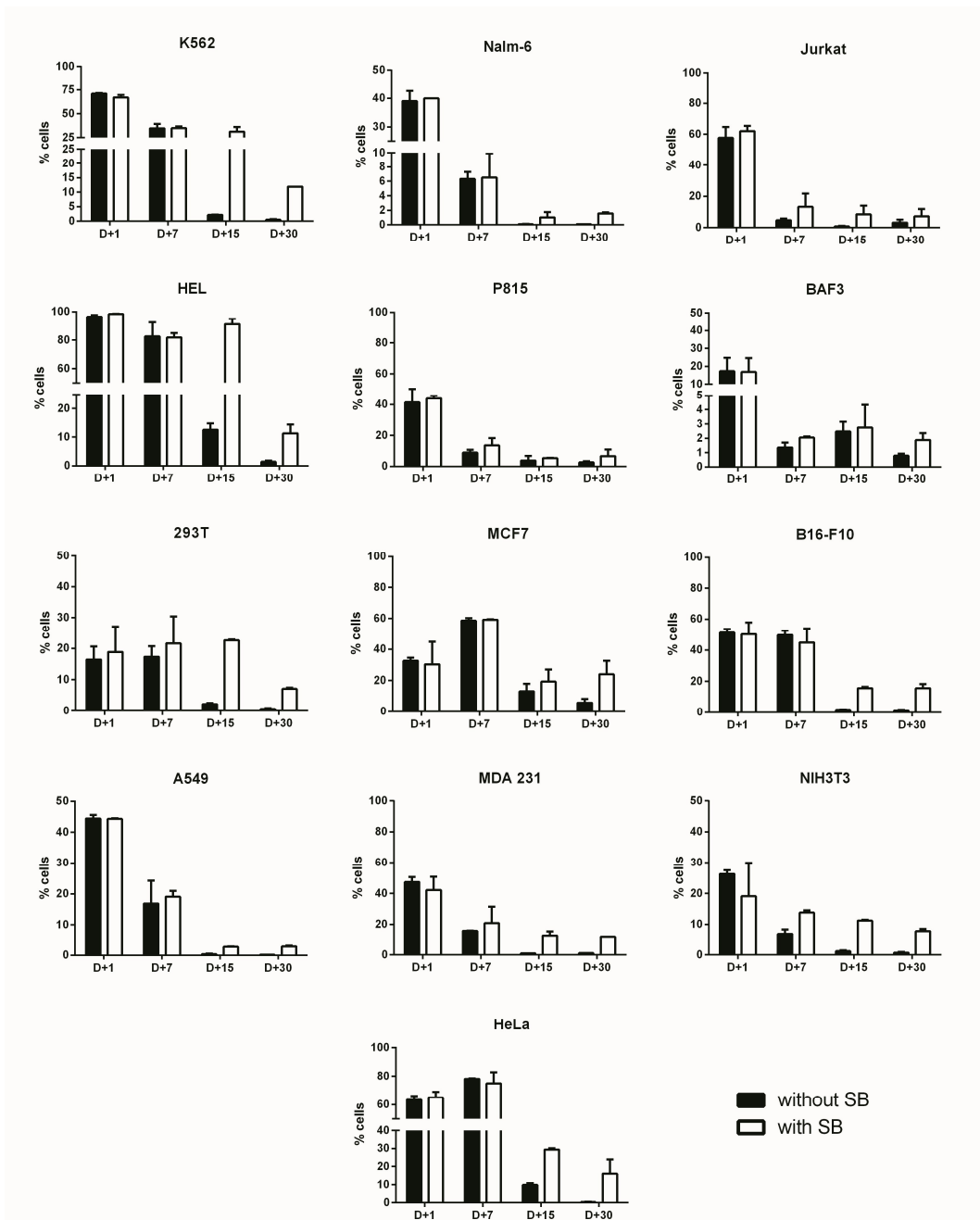
381





382  
383

384 **Figure 2: Electroporation score for cell lines.** Cell lines were electroporated with pT2-  
 385 GFP (4ug) using each one of the seven buffers and the recommended program. Viability  
 386 (blue bar), GFP expression (green bar) and electroporation score (red bar) were assessed  
 387 one day after nucleofection (d+1). Viability data were normalized with viability from  
 388 non-transfected cells. Data are shown as mean  $\pm$  SD from three experiments performed  
 389 in duplicate and were further analyzed using one-way ANOVA with Tukey's multiple  
 390 comparisons test. Significant differences ( $p < 0,05$ ) are depicted in the table next to each  
 391 graph, with each color denoting one parameter.  
 392



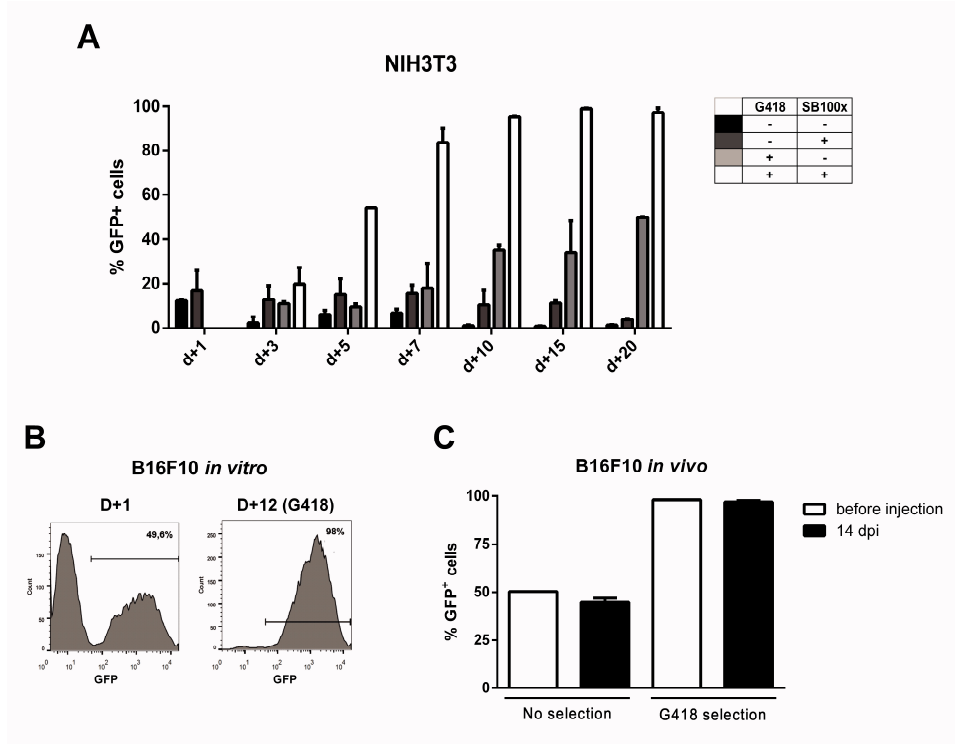
393  
394  
395  
396  
397  
398  
399  
400

**Figure 3: Long term transgene expression in electroporated cell lines using SB system.** Cell lines were electroporated with pT2-GFP (4ug) using the combination of buffer and program indicated on table 1, with (white bar) or without (black bar) the addition of SB100x transposase (1ug). GFP expression was analyzed until d+30 for each cell line. Data are shown as mean  $\pm$  SD from one single experiment performed in duplicate.

401  
402  
403

For fast and easy enrichment of GFP-positive cells we constructed a bidirectional vector encoding GFP and G418 resistance in the backbone of pT3 transposon, named pT3-Neo-EF1a-GFP. Indeed, the expression level obtained after nucleofection was

404 sufficient to select G418-resistant clones after electroporation with this plasmid, as shown  
 405 for NIH3T3 (Fig. 4A) and B16F10 (Fig. 4B) cell lines. After G418 selection and  
 406 withdrawal, GFP expression remained stable in NIH3T3 cells for 15 days (Figure S15).  
 407 Furthermore, when the modified B16F10 cells were injected *in vivo* and allowed to form  
 408 subcutaneous tumors, the cells extracted from the tumor at d+14 post inoculation (dpi)  
 409 still expressed high levels of GFP, indicating that the transgenic cassette is integrated in  
 410 the genome and has stable expression, with no signs of *in vivo* silencing of the transgene  
 411 (Figs. 4C and Figure S16).



412

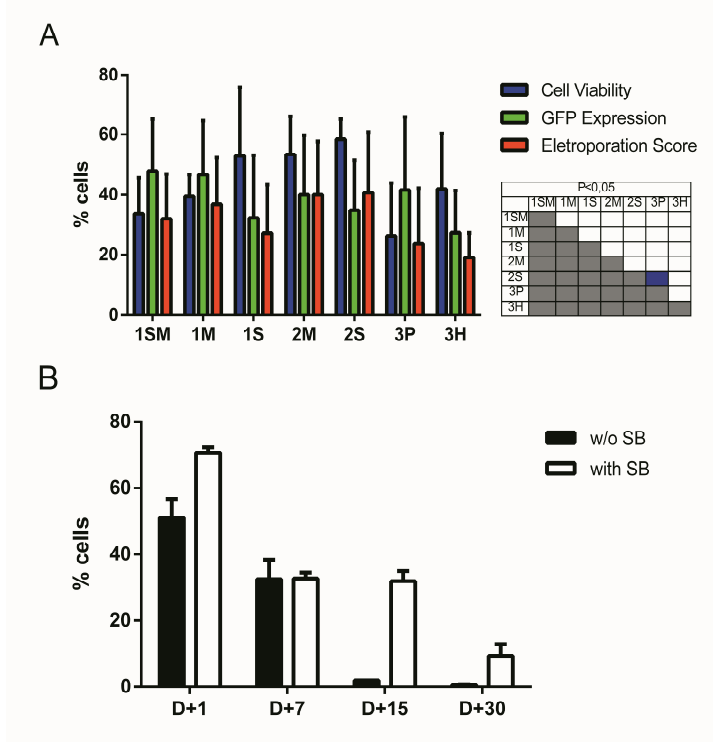
413 **Figure 4: Transgene expression can be enriched by using G418 and is retained after**  
 414 ***in vivo* growth.** Using the programs and buffers indicated on table 1, NIH3T3 (A) and  
 415 B16F10 (B) cell lines were electroporated. G418 was added two days after nucleofection  
 416 and GFP expression was accompanied until d+20 (NIH3T3) or d+12 (B16F10). (C)  $5 \times 10^5$   
 417 B16F10 cells submitted or not to selection with G418 were injected in the left flank of  
 418 C57Bl/6 mice. Tumors were extracted 14 days post injection (dpi), cells were passed *in*  
 419 *vitro* for one week and GFP expression analyzed by FACS.

420 Variations of the pT3-Neo-EF1a-GFP construct were developed, such as the pT3-  
 421 Neo plasmid, which confers resistance to G418 antibiotic and has restriction sites that  
 422 allow cloning of a second expression cassette. This plasmid was validated in G418  
 423 resistance assays using B16F10 cells (data not shown). The map for this plasmid is shown  
 424 in Figure S18.

425

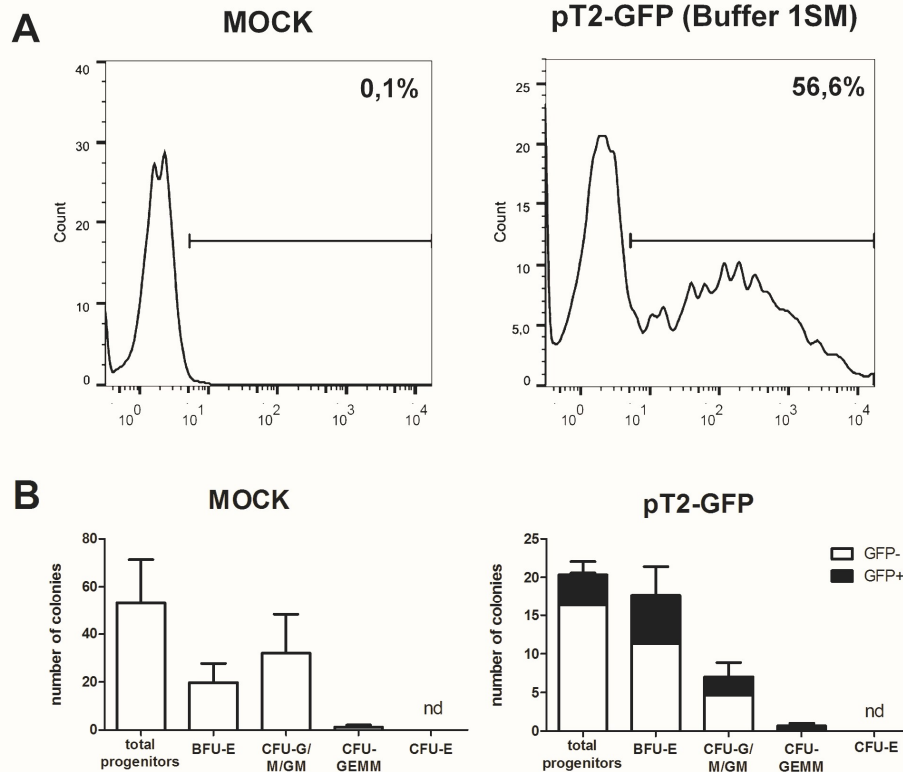
426 The use of primary cells derived from patients or healthy donors provides a more  
 427 accurate model for *in vitro* and *in vivo* experiments, and these cells can also be used in  
 428 cell therapy approaches to treat a large number of diseases. However, these applications  
 429 often depend on genetic modification, which is usually hard to perform in these cells. To  
 430 evaluate the performance of Chicabuffers in the gene transfer to these cells, we isolated  
 431 adipose tissue derived MSCs and cord blood purified CD34<sup>+</sup> hematopoietic stem cells

432 and electroporated the cells with the plasmids pT2-GFP and SB100x. As shown in figure  
 433 5A, the best electroporation score for MSC was obtained using buffer 2S, with 57% of  
 434 viable cells and 39% of GFP expression. When using SB100X, long-term expression of  
 435 GFP using this buffer was seen in 12% of cells (Fig. 5B). For CD34+ cells, around 57%  
 436 were GFP-positive one day after electroporation using buffer 1SM and program U-008  
 437 (Fig. 6A). These cells were plated in methylcellulose-based medium, allowing long-term  
 438 assessment of GFP expression and differentiation potential. After three weeks, GFP+  
 439 CD34+ cells were able to differentiate to erythroid, granulocytic and myeloid lineages  
 440 (Fig. 6B), showing that the insertion of the transgene did not affect the stemness of the  
 441 cells and that differentiated cells display high GFP expression (Figure S17).



442

443 **Figure 5: SB based GFP gene transfer to adipose tissue derived human MSCs.** (A)  
 444 MSCs were electroporated with each one of the seven buffers and the recommended  
 445 program. Viability (blue bar), GFP expression (green bar) and electroporation score (red  
 446 bar) were assessed one day after nucleofection (d+1). (B) Long term GFP expression was  
 447 evaluated until d+30 post nucleofection with (white bar) or without (black bar) the  
 448 addition of SB100x transposase (1ug per cuvette). Data are shown as mean  $\pm$  SD from  
 449 three experiments performed in duplicate and were further analyzed using one-way  
 450 ANOVA with Tukey's multiple comparisons test. Significant differences ( $p < 0,05$ ) are  
 451 depicted in the table next to each graph, with each color denoting one parameter.



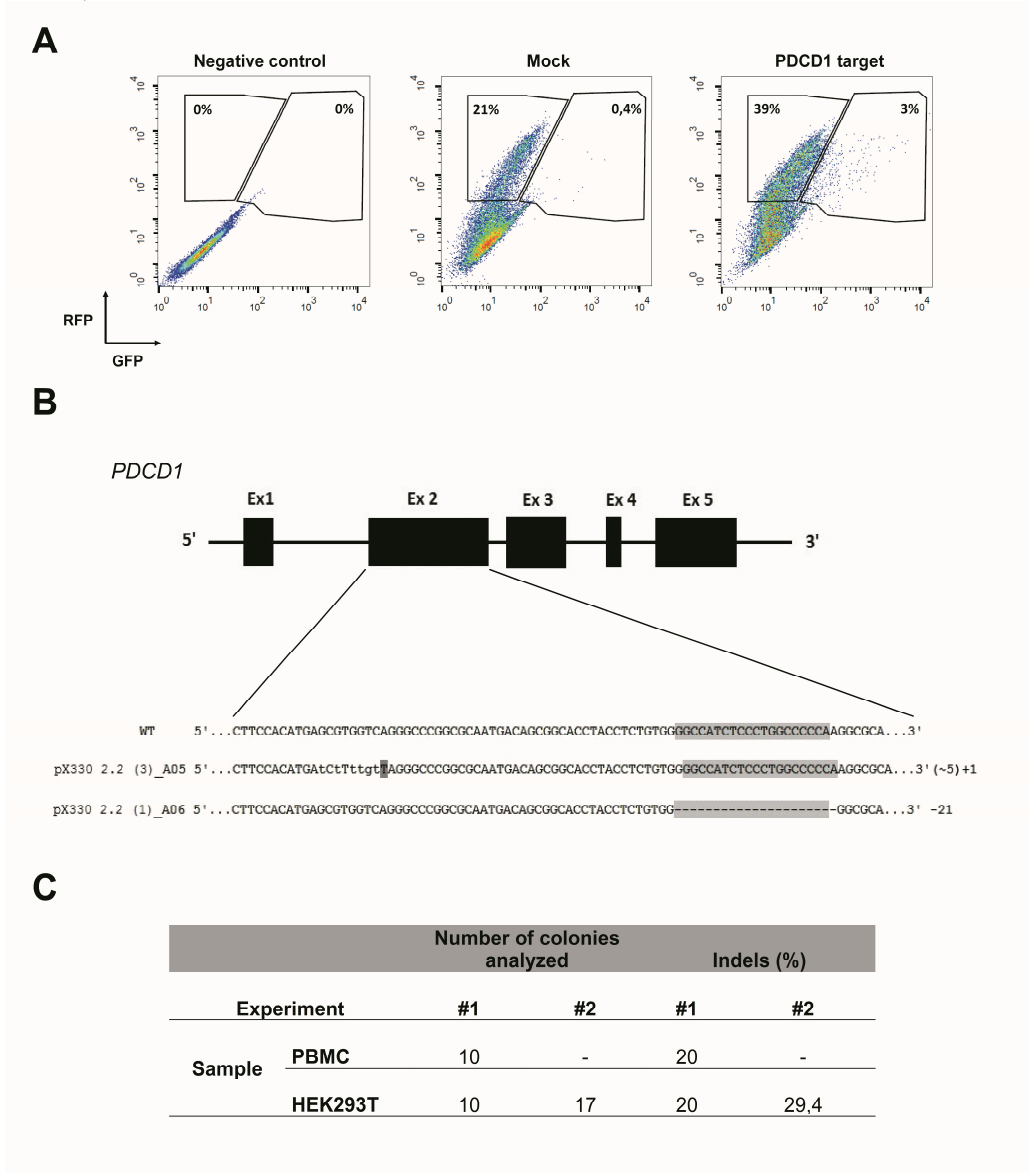
452

453 **Figure 6: SB based GFP gene transfer to human cord blood CD34+ cells.** (A) GFP  
 454 expression in CD34+ cells electroporated with plasmids pT2-GFP (4ug) and SB100x  
 455 (1ug) using program U-008 and buffer 1SM. GFP expression was evaluated by FACS at  
 456 d+1 post nucleofection. (B) Electroporated cells ( $2 \times 10^3$  per well) were plated in  
 457 methylcellulose media and allowed to differentiate for 3 weeks. Colonies were quantified  
 458 for mock (left) and GFP electroporated (right) cells. GFP positive colonies (black bars)  
 459 were determined within total colonies identified. CFU-E: colony forming unit – erythroid;  
 460 BFU-E: burst forming unit – erythroid; CFU-G/M/GM: colony forming unit –  
 461 granulocyte/monocyte/; CFU-GEMM: colony forming unit – granulocyte-erythrocyte-  
 462 monocyte-megakaryocyte. Data are shown as mean  $\pm$  SD from two experiments.

463

464 The recent description of the CRISPR/Cas9 system as an efficient tool to edit the  
 465 genome of cells has clear implications for basic cell biology studies and gene therapy  
 466 protocols (Doudna and Charpentier, 2014). To achieve efficient gene editing of target  
 467 cells, Cas9 nuclease and the guide RNA (gRNA) must be expressed in the cell, ideally in  
 468 a transient fashion. To evaluate the efficiency of Chicabuffers in promoting Cas9  
 469 mediated genome editing, we designed a gRNA targeting exon 2 of *PDCD1* gene, which  
 470 encodes the inhibitory receptor PD-1, a relevant potential target for cancer cell based  
 471 immunotherapy (Chicaybam and Bonamino, 2014; Hamid et al., 2013). For the validation  
 472 of gRNA, we used plasmid pRGS-CR-PDCD1, which has the *PDCD1* target sequence  
 473 cloned between a red fluorescent protein (RFP) and a GFP, resulting in an out-of-frame  
 474 GFP. In this system, GFP expression can be restored by CRISPR-mediated non-  
 475 homologous end joining (NHEJ) repair (Kim et al., 2011), leading to restoration of the  
 476 reading frame in nearly 1/3 of the editions. Co-electroporation of 293T cells with the

477 report construct and the plasmid carrying CRISPR/Cas9/gRNA, but not CRISPR/Cas9  
 478 lacking the gRNA sequence, resulted in GFP expression in approximately 7% of the  
 479 RFP+ cells (3% out of 42%), indicating that sequence-specific DNA editing was achieved  
 480 (Fig. 7A). A similar approach was performed in PBMCs and following electroporation,  
 481 indels were verified by amplification of *PDCD1* locus of the edited cells, which was  
 482 subsequently cloned in pCR2.1 vector and analyzed by Sanger sequencing, evidencing  
 483 cells containing indels of varying lengths in the *PDCD1* locus (Fig. 7B). The results of  
 484 gene editing experiments in 293T and PBMCs are summarized in figure 7C. The  
 485 characterization of indels in PBMCs and 293T cells indicate that the use of our optimized  
 486 electroporation protocol allowed efficient editing of *PDCD1* locus in the tested samples.  
 487 All the indels led to disruptions of the reading frame of the PD1 sequence (data not  
 488 shown).



489

490 **Figure 7: Electroporation of CRISPR/Cas9 cassettes promotes gene editing of**  
 491 **PBMCs and 293T cells.** (A) 293T cells were electroporated (buffer 3P, program A-023)  
 492 without plasmid (negative control), with pRGS-CR plasmid (without *PDCD1* target

493 sequence; mock) or with pRGS-CR-PDCD1. GFP and RFP expression was analyzed 24  
 494 hours later. Numbers depict the percentage of cells inside each gate. (B) Representative  
 495 image showing indels obtained in *PDCD1* gene after electroporation of PBMCs with  
 496 plasmid px330 (Cas9/gRNA). The indels are represented by lower case characters;  
 497 numbers inside parenthesis depict substitutions (~) and numbers outside parenthesis  
 498 depict additions (+) or deletions (-). Exons are not draw into scale. (C) Summarized  
 499 results obtained for 293T cells and PBMCs, showing the number of colonies sequenced  
 500 and the percentage of indels detected. Two experiments were done for each cell.

501 Multiple target editing is possible using CRISPR systems. Since multiple loci  
 502 editing require multiple gRNA, we evaluated the possibility of co-electroporating PBMCs  
 503 with a reporter plasmid and FITC labeled short RNAs. This setting could be used to co-  
 504 electroporate a plasmid encoding a reporter gene (or Cas9 nuclease) and multiple short  
 505 RNAs (such as gRNAs for editing several loci). Using the buffer 3P we were able to  
 506 achieve high viability (Figure S19a) and up to 60,7% of cells expressing the short RNA  
 507 when 50pmol of the RNA were used (Figure S19b). Concentrations above 75pmol of  
 508 short RNA resulted in increased cell death and were not further used (data not show).  
 509 From electroporated cells under the same condition, up to 14,8% co-expressed the  
 510 reporter plasmid (encoding RFP) and the labeled short RNA (Figure S19c). This setting  
 511 clearly allows efficient co-electroporation of plasmid DNA and short RNA, opening the  
 512 possibility of combining siRNA and transgene expression or even multiple gRNAs and  
 513 Cas9 expressing plasmids for gene editing.

514

515 **Table 1: Summarized electroporation conditions for each cell line (based in figure**  
 516 **2; d1 after electroporation).**

517

Cell Line	Cell Type	Program	Recommended Buffer	Viability (Chicabuffer; $\pm$ SD)	Viability (Lonza)	GFP expression (Chicabuffer)	GFP expression (Lonza)
<u>Non-adherent</u>							
BA/F3	Mouse pro B cell	X-001	2M	91,8 $\pm$ 2,7 %	79,00 %	55,05 $\pm$ 14,2 %	88,00 %
HEL	Erythroleukemia; erythroblast cell	X-005	1S	70,4 $\pm$ 17,1 %	39-66 %	79 $\pm$ 6,2 %	94,00 %
Jurkat	Acute T cell leukemia, T lymphocyte; lymphoblastoid cells	X-001	1SM	75,7 $\pm$ 6,8 %	90,00 %	69 $\pm$ 11,6 %	88,00 %

K562	Human chronic myelogenous leukemia; lymphoblastoid cells	T016	1M	70,7±13,8 %	88,00 %	64,1±8%	80-90%
Nalm-6	Human B cell precursor leukemia	C-005	3P	74,2±11,8 %	87,00 %	40,6±14,7 %	64,00%
P815	Mouse mastocytoma; mast cells	C-005	3P	70,2±29,9 %	92,00 %	60,5±16,6 %	62,00%
<u>Adherent</u>							
A549	Human lung carcinoma; epithelial cells	X-001	3P	59,4±27,3 %	81,00 %	63,5±11,4 %	72,00%
293T	Human embryonal kidney; adherent fibroblastoid cells	A-023	1SM	79,9±24,7 %	90,00 %	38,6±30,2 %	90,00%
B16F10	Mouse skin melanoma	P-020	2S	39,9±17 %	91,00 %	49,3±15,7 %	84,00%
HeLa	Human cervix carcinoma; epitheloid cells in monolayers	I-013	1M	45,1±16,5 %	85-90%	66,4±8,3 %	70,00%
MCF7	Human breast adenocarcinoma; epithelial cells	P-020	1M	68,4±10,9 %	60,00 %	57±23,3 %	77,00%



MDA- MB- 231	Human breast adenocarcinoma; epithelial cells	X-013	1SM	85,6±15 %	77,00 %	48,5±17,5 %	79,00%
human MSCs	Human mesenchymal stem cells	U-023	2S	58,5±6,8 %	48,00 %	35±16,6 %	80,00%
NIH3 T3	NIH Swiss mouse embryo; adherent fibroblastoid cells	U-030	1SM	49,4±30,4 %	87,00 %	52,5±19,5 %	84,00%

## 518 Discussion

519

520

521

522

523

524

525

526

527

528

529

530

531

532

533

534

535

536

537

538

539

540

541

542

543

544

545

546

547

548

Genetic modification of cells is a cumbersome and expensive process, often involving the use of viral vectors to achieve high efficiency transgene expression. The use of electroporation for the genetic modification of cells is being adopted by many laboratories as it represents a fast and cheap option for transfer of plasmids and RNA. Moreover, this technique is also very efficient, inducing transgene expression levels comparable to viral vectors in some cells (Bilal et al., 2015). Equipments capable of generating square-wave voltage pulses, like Lonza Nucleofector, are among the most efficient for mammalian cell electroporation (Mir, 2014). However, costs associated with the acquisition of nucleofection kits, especially if used in a routine basis, might hamper the use of this technology in some laboratories or impair large-scale experiments.

In a previous work, our group described seven in house buffers and tested the electroporation efficiency of Jurkat cells and primary lymphocytes using Nucleofector (Chicaybam et al., 2013). The selected buffers induced high transgene expression and low toxicity, comparable to results obtained when Lonza's kit were used. In this context, the present work comprises a practical guide for the electroporation of 14 cell lines and primary MSCs and HSCs, determining the best buffer (among seven options) to be used with Lonza Nucleofector II, a widely disseminated electroporation device. The electroporation score calculated for every cell line is a general guide for electroporation efficiency comparison, and the buffer choice can be adapted to the need of the planned experiment (higher GFP expression or cell viability). Chicabuffers showed to work for all the cells tested with most of the samples showing interchangeable results among the different buffers and only few exceptions where one of the buffers performed poorly. This results place Chicabuffers as a valuable tool for cheap and fast gene modification of basically every cell tested. Although we focused in Lonza's device, it is likely that a similar approach using these buffers in conjunction with electroporators that allow modification of electroporation conditions could achieve even better results by fine tuning parameters like pulse amplitude, voltage and wave forms (Yarmush et al., 2014). Lonza's buffers were already described to have good results when tested with alternative

549 nucleofector Iib programs (Gresch et al., 2004), suggesting that there is still room for  
550 optimization of electroporation conditions, reinforcing the potential of testing  
551 Chicabuffers under different experimental settings.

552

553 Short-term viability and expression of GFP was very efficient for the majority of  
554 cell lines, and Chicabuffers performed equally well when compared to the results reported  
555 by Lonza, especially for non-adherent cell lines (table 1 and Fig. 2). Furthermore, our  
556 results are comparable to those reported in the literature for cell lines like K562 (Gresch  
557 et al., 2004) primary MSCs (Aluigi et al., 2006), although direct comparison of the results  
558 must be taken carefully because different plasmids were used. By combining this strategy  
559 with the Sleeping Beauty transposon system, the provided optimized protocols allowed  
560 long-term expression of transgenes in all the cells tested (Fig. 3). In the case of viral  
561 vectors, especially retroviral and lentiviral vectors, there is a wide availability of  
562 constructs carrying selectable markers, fluorescent reporters, promoters for different  
563 finalities and cassette configurations, increasing the options of possible cellular  
564 manipulations (Szulc et al., 2006; Vargas et al., 2012; Weber et al., 2008). This is in sharp  
565 contrast to the Sleeping Beauty system, which has a limited offer of transfer plasmids  
566 available. The new vectors developed and validated in the present report can improve  
567 flexibility and increase the applicability of this system, promoting accessible and efficient  
568 transgene integration into different cell types. These plasmids showed high and stable  
569 levels of transgene expression, and the addition of antibiotic resistance allowed the  
570 selection of GFP-expressing clones in vitro. Long-term expression of the transgene can  
571 be potentially increased by the use of SB100x RNA, decreasing the toxicity of the  
572 electroporation process as reported (Peng et al., 2009), or by carefully titrating the  
573 transposase plasmid mass to avoid overproduction inhibition (Grabundzija et al., 2010).  
574 These vectors and others recently reported in the literature (Kowarz et al., 2015), in  
575 conjunction with Chicabuffers, could be potentially used in diverse experimental gene  
576 therapy approaches, such as T cell immunotherapy (Singh et al., 2015), MSC (Martin et  
577 al., 2014) and stem cell gene therapy protocols (Aiuti et al., 2013), further facilitating the  
578 application of these technologies in basic, translational and clinical studies.

579

580 Our results show the feasibility of this approach, enabling a stable transgene  
581 expression in CD34+ cells from cord blood samples, keeping GFP expression throughout  
582 hematopoietic differentiation. It would be interesting to test this strategy in stem cell  
583 differentiation models other than the hematopoietic system such as the central nervous  
584 system (Sartore et al., 2011), including models of in vivo differentiation. In addition, cells  
585 with clear therapeutic potential, such as T lymphocytes (Chicaybam et al., 2013) and  
586 MSCs (this report) could be stably modified using a combination of Chicabuffer, SB and  
587 electroporation.

588

589 SB mediated modification of cells as described here proved to be stable in vitro  
590 and in vivo, with cells retaining transgene expression during tumor development in  
591 immunocompetent mice. The GFP+ B16F10 cells not only retained GFP expression level,  
592 but also kept a constant ratio of GFP+/GFPneg cells throughout the 15-day period of in  
593 vivo tumor development. This result suggests that no gene silencing occurs for the SB  
594 transgenic cassette, supporting in vivo utilization of this tool, as described elsewhere  
595 (Belur et al., 2003; Hausl et al., 2010).

596

597 Furthermore, we showed efficient CRISPR-mediated genome editing of *PDCD1*  
598 gene in 293T and human PBMCs electroporated using Chicabuffers. Designing a single

599 plasmid encoding Cas9+gRNA is simpler than constructing zinc finger nuclease (Beane  
600 et al., 2015) or TALEN (Berdien et al., 2014) based cassettes. The single plasmid  
601 approach for PBMC edition is also simpler to assemble than the recently reported  
602 Cas9+gRNA ribonucleoproteins (Schumann et al., 2015), showing that our extremely  
603 simple protocol can be used to edit cell genomes. The gRNA used for *PDCD1* locus  
604 edition in our report targets exon 2, in contrast to exon 1 editions promoted by Schumann  
605 et al [42], showing that different gRNAs can be used to efficiently disrupt the *PDCD1*  
606 gene sequence. The levels of gene editing obtained with our approach allow similar  
607 downstream applications in primary lymphocytes as those proposed by the above  
608 mentioned reports, but with a reduced effort to design the gene editing tool (plasmid bases  
609 CRISPR system vs TALEN or ZFN) or the electroporation reagents (plasmid vs  
610 RNA+protein). Furthermore, the protocol described for the co-electroporation of short  
611 RNAs and plasmids carrying GFP+Cas9 can be exploited for multiple loci editing in  
612 PBMCs, opening the possibility of targeting simultaneously several genes of interest.

613

614 In summary, our study describes general guidelines for the efficient  
615 electroporation of primary mammal cells and several cell lines. Furthermore, our data  
616 validates a series of flexible SB-based plasmids for the integration of transgenes and  
617 downstream selection of gene-modified cells. The combination of transposon,  
618 Chicabuffers and electroporation, as described here, represents a straightforward  
619 approach for transient gene expression and permanent gene modification of cell lines and  
620 human primary cells.

621

#### 622 **List of abbreviations**

623 CRISPR: clustered regularly interspaced short palindromic repeats

624 TALEN: Transcription activator-like effector nucleases

625 PBMC: peripheral blood mononuclear cells

626 MSC: mesenchymal stem cells

627 GFP: green fluorescent protein

628 RFP: red fluorescent protein

629 7-AAD: 7-amoniactinomycin D

630 ITR: inverted terminal repeats

631 SB: sleeping beauty transposase

632 Dpi: days post inoculation

633 gRNA: guide RNA

634 NHEJ: non-homologous end joining

635 FITC: Fluorescein isothiocyanate

636 HSC: human stem cell

637

638

#### 639 **Competing interests**

640

641 The authors declare that they have no competing interests

642

#### 643 **Funding**

644

645 This work was supported by grants from Conselho Nacional de Desenvolvimento  
646 Científico e Tecnológico (CNPq), Fundação de Amparo à Pesquisa do Estado do Rio de  
647 Janeiro (FAPERJ), Coordenação de Aperfeiçoamento de Pessoal de Nível Superior

648 (CAPES), Brazilian National Cancer Institute (INCA) and Oncobiology  
649 program/Universidade Federal do Rio de Janeiro (UFRJ).

650

### 651 **Authors' contributions**

652

653 LC, CB, BP, MC, PR and LB performed the electroporation experiments (cell lines,  
654 MSCs and PBMCs), data analysis and interpretation. CGL, CL, FRB and ZV performed  
655 electroporation and differentiation experiments in CD34+ cells, data analysis and  
656 interpretation. LC and MHB took part in the conception and design of the study, data  
657 interpretation and manuscript writing. All authors read and approved the final manuscript.

658

### 659 **Acknowledgments**

660

661 We thank Sang Wang Han (UNIFESP – Brazil) for pT2-GFP and SB100x plasmids,  
662 Richard Morgan (NIH) for pT3-GFP plasmid and Amilcar Tanuri (UFRJ) for pRGS-CR  
663 plasmid. We also thank all the researchers that provided the cell lines used in this study.

664

665

### 666 **References**

667

668 Aiuti, A., Biasco, L., Scaramuzza, S., Ferrua, F., Cicalese, M. P., Baricordi, C., et al.  
669 (2013). Lentiviral hematopoietic stem cell gene therapy in patients with Wiskott-  
670 Aldrich syndrome. *Science* 341, 1233151. doi:10.1126/science.1233151.

671 Aluigi, M., Fogli, M., Curti, A., Isidori, A., Gruppioni, E., Chiodoni, C., et al. (2006).  
672 Nucleofection is an efficient nonviral transfection technique for human bone  
673 marrow-derived mesenchymal stem cells. *Stem Cells* 24, 454–461.  
674 doi:10.1634/stemcells.2005-0198.

675 Barretina, J., Caponigro, G., Stransky, N., Venkatesan, K., Margolin, A. A., Kim, S., et  
676 al. (2012). The Cancer Cell Line Encyclopedia enables predictive modelling of  
677 anticancer drug sensitivity. *Nature* 483, 603–607. doi:10.1038/nature11003.

678 Beane, J. D., Lee, G., Zheng, Z., Mendel, M., Abate-Daga, D., Bharathan, M., et al.  
679 (2015). Clinical Scale Zinc Finger Nuclease-mediated Gene Editing of PD-1 in  
680 Tumor Infiltrating Lymphocytes for the Treatment of Metastatic Melanoma. *Mol.*  
681 *Ther.* 23, 1380–1390. doi:10.1038/mt.2015.71.

682 Behr, J.-P. (2012). Synthetic gene transfer vectors II: back to the future. *Acc. Chem. Res.*  
683 45, 980–984. doi:10.1021/ar200213g.

684 Belur, L. R., Frandsen, J. L., Dupuy, A. J., Ingbar, D. H., Largaespada, D. A., Hackett, P.  
685 B., et al. (2003). Gene insertion and long-term expression in lung mediated by the  
686 Sleeping Beauty transposon system. *Mol. Ther.* 8, 501–507. doi:10.1016/S1525-  
687 0016(03)00211-9.

688 Berdien, B., Mock, U., Atanackovic, D., and Fehse, B. (2014). TALEN-mediated editing  
689 of endogenous T-cell receptors facilitates efficient reprogramming of T lymphocytes  
690 by lentiviral gene transfer. *Gene Ther.* 21, 539–548. doi:10.1038/gt.2014.26.

691 Bilal, M. Y., Vacaflares, A., and Houtman, J. C. (2015). Optimization of methods for the  
692 genetic modification of human T cells. *Immunol. Cell Biol.* 93, 896–908.  
693 doi:10.1038/icb.2015.59.

694 Blower, P. E., Verducci, J. S., Lin, S., Zhou, J., Chung, J.-H., Dai, Z., et al. (2007).  
695 MicroRNA expression profiles for the NCI-60 cancer cell panel. *Mol. Cancer Ther.*  
696 6, 1483–1491. doi:10.1158/1535-7163.MCT-07-0009.

- 697 Bonamino, M., Serafini, M., D'Amico, G., Gaipa, G., Todisco, E., Bernasconi, S., et al.  
698 (2004). Functional transfer of CD40L gene in human B-cell precursor ALL blasts  
699 by second-generation SIN lentivectors. *Gene Ther.* 11, 85–93.  
700 doi:10.1038/sj.gt.3302141.
- 701 Chicaybam, L., and Bonamino, M. H. (2014). Moving receptor redirected adoptive cell  
702 therapy toward fine tuning of antitumor responses. *Int. Rev. Immunol.* 33, 402–416.  
703 doi:10.3109/08830185.2014.917412.
- 704 Chicaybam, L., Sodre, A. L., Curzio, B. A., and Bonamino, M. H. (2013). An efficient  
705 low cost method for gene transfer to T lymphocytes. *PLoS One* 8, e60298.  
706 doi:10.1371/journal.pone.0060298.
- 707 Doudna, J. A., and Charpentier, E. (2014). Genome editing. The new frontier of genome  
708 engineering with CRISPR-Cas9. *Science* 346, 1258096.  
709 doi:10.1126/science.1258096.
- 710 Faget, D. V., Lucena, P. I., Robbs, B. K., and Viola, J. P. B. (2012). NFAT1 C-terminal  
711 domains are necessary but not sufficient for inducing cell death. *PLoS One* 7,  
712 e47868. doi:10.1371/journal.pone.0047868.
- 713 Gillet, J.-P., Varma, S., and Gottesman, M. M. (2013). The clinical relevance of cancer  
714 cell lines. *J. Natl. Cancer Inst.* 105, 452–458. doi:10.1093/jnci/djt007.
- 715 Grabundzija, I., Irgang, M., Mátés, L., Belay, E., Matrai, J., Gogol-Döring, A., et al.  
716 (2010). Comparative analysis of transposable element vector systems in human cells.  
717 *Mol. Ther.* 18, 1200–1209. doi:10.1038/mt.2010.47.
- 718 Gresch, O., Engel, F. B., Nesic, D., Tran, T. T., England, H. M., Hickman, E. S., et al.  
719 (2004). New non-viral method for gene transfer into primary cells. *Methods* 33, 151–  
720 163. doi:10.1016/j.ymeth.2003.11.009.
- 721 Griffin, J. L., and Shockcor, J. P. (2004). Metabolic profiles of cancer cells. *Nat. Rev.*  
722 *Cancer* 4, 551–561. doi:10.1038/nrc1390.
- 723 Hamid, O., Robert, C., Daud, A., Hodi, F. S., Hwu, W.-J., Kefford, R., et al. (2013).  
724 Safety and Tumor Responses with Lambrolizumab (Anti-PD-1) in Melanoma. *N.*  
725 *Engl. J. Med.* 369, 134–144. doi:10.1056/NEJMoa1305133.
- 726 Hausl, M. A., Zhang, W., Müther, N., Rauschhuber, C., Franck, H. G., Merricks, E. P., et  
727 al. (2010). Hyperactive sleeping beauty transposase enables persistent phenotypic  
728 correction in mice and a canine model for hemophilia B. *Mol. Ther.* 18, 1896–1906.  
729 doi:10.1038/mt.2010.169.
- 730 Jinek, M., Chylinski, K., Fonfara, I., Hauer, M., Doudna, J. A., and Charpentier, E.  
731 (2012). A programmable dual-RNA-guided DNA endonuclease in adaptive bacterial  
732 immunity. *Science* 337, 816–821. doi:10.1126/science.1225829.
- 733 Jordan, M., and Wurm, F. (2004). Transfection of adherent and suspended cells by  
734 calcium phosphate. *Methods* 33, 136–143. doi:10.1016/j.ymeth.2003.11.011.
- 735 Kim, H., and Kim, J.-S. (2014). A guide to genome engineering with programmable  
736 nucleases. *Nat. Rev. Genet.* 15, 321–334. doi:10.1038/nrg3686.
- 737 Kim, H., Um, E., Cho, S.-R., Jung, C., Kim, H., and Kim, J.-S. (2011). Surrogate reporters  
738 for enrichment of cells with nuclease-induced mutations. *Nat. Methods* 8, 941–943.  
739 doi:10.1038/nmeth.1733.
- 740 Kotnik, T., Frey, W., Sack, M., Haberl Meglič, S., Peterka, M., and Miklavčič, D. (2015).  
741 Electroporation-based applications in biotechnology. *Trends Biotechnol.* 33, 480–  
742 488. doi:10.1016/j.tibtech.2015.06.002.
- 743 Kowarz, E., Löscher, D., and Marschalek, R. (2015). Optimized Sleeping Beauty  
744 transposons rapidly generate stable transgenic cell lines. *Biotechnol. J.* 10, 647–653.  
745 doi:10.1002/biot.201400821.

- 746 Kuystermans, D., and Al-Rubeai, M. (2015). “Biopharmaceutical Products from Animal  
747 Cell Culture,” in *Animal Cell Culture Cell Engineering*. (Springer International  
748 Publishing), 717–757. doi:10.1007/978-3-319-10320-4\_23.
- 749 Martin, P. K. M., Stilhano, R. S., Samoto, V. Y., Takiya, C. M., Peres, G. B., da Silva  
750 Michelacci, Y. M. C., et al. (2014). Mesenchymal stem cells do not prevent antibody  
751 responses against human  $\alpha$ -L-iduronidase when used to treat mucopolysaccharidosis  
752 type I. *PLoS One* 9, e92420. doi:10.1371/journal.pone.0092420.
- 753 Mátés, L., Chuah, M. K. L., Belay, E., Jerchow, B., Manoj, N., Acosta-Sanchez, A., et al.  
754 (2009). Molecular evolution of a novel hyperactive Sleeping Beauty transposase  
755 enables robust stable gene transfer in vertebrates. *Nat. Genet.* 41, 753–761.  
756 doi:10.1038/ng.343.
- 757 Mir, L. M. (2014). Electroporation-based gene therapy: recent evolution in the  
758 mechanism description and technology developments. *Methods Mol. Biol.* 1121, 3–  
759 23. doi:10.1007/978-1-4614-9632-8\_1.
- 760 Nishizuka, S., Charboneau, L., Young, L., Major, S., Reinhold, W. C., Waltham, M., et  
761 al. (2003). Proteomic profiling of the NCI-60 cancer cell lines using new high-  
762 density reverse-phase lysate microarrays. *Proc. Natl. Acad. Sci. U. S. A.* 100,  
763 14229–14234. doi:10.1073/pnas.2331323100.
- 764
- 765 Optimized CRISPR Design Available at: <http://crispr.mit.edu/> [Accessed July 29, 2016].  
766
- 767 Park, E. S., Rabinovsky, R., Carey, M., Hennessy, B. T., Agarwal, R., Liu, W., et al.  
768 (2010). Integrative analysis of proteomic signatures, mutations, and drug  
769 responsiveness in the NCI 60 cancer cell line set. *Mol. Cancer Ther.* 9, 257–267.  
770 doi:10.1158/1535-7163.MCT-09-0743.
- 771 Peng, P. D., Cohen, C. J., Yang, S., Hsu, C., Jones, S., Zhao, Y., et al. (2009). Efficient  
772 nonviral Sleeping Beauty transposon-based TCR gene transfer to peripheral blood  
773 lymphocytes confers antigen-specific antitumor reactivity. *Gene Ther.* 16, 1042–  
774 1049. doi:10.1038/gt.2009.54.
- 775 Ramanayake, S., Bilton, I., Bishop, D., Dubosq, M.-C., Blyth, E., Clancy, L., et al.  
776 (2015). Low-cost generation of Good Manufacturing Practice-grade CD19-specific  
777 chimeric antigen receptor-expressing T cells using piggyBac gene transfer and  
778 patient-derived materials. *Cytotherapy* 17, 1251–1267.  
779 doi:10.1016/j.jcyt.2015.05.013.
- 780 Sartore, R. C., Campos, P. B., Trujillo, C. A., Ramalho, B. L., Negraes, P. D., Paulsen,  
781 B. S., et al. (2011). Retinoic acid-treated pluripotent stem cells undergoing  
782 neurogenesis present increased aneuploidy and micronuclei formation. *PLoS One* 6,  
783 e20667. doi:10.1371/journal.pone.0020667.
- 784 Satkauskas, S., Ruzgys, P., and Venslauskas, M. S. (2012). Towards the mechanisms for  
785 efficient gene transfer into cells and tissues by means of cell electroporation. *Expert*  
786 *Opin. Biol. Ther.* 12, 275–286. doi:10.1517/14712598.2012.654775.
- 787 Schumann, K., Lin, S., Boyer, E., Simeonov, D. R., Subramaniam, M., Gate, R. E., et al.  
788 (2015). Generation of knock-in primary human T cells using Cas9  
789 ribonucleoproteins. *Proc. Natl. Acad. Sci. U. S. A.* 112, 10437–10442.  
790 doi:10.1073/pnas.1512503112.
- 791 Singh, H., Moyes, J. S. E., Huls, M. H., and Cooper, L. J. N. (2015). Manufacture of T  
792 cells using the Sleeping Beauty system to enforce expression of a CD19-specific  
793 chimeric antigen receptor. *Cancer Gene Ther.* 22, 95–100. doi:10.1038/cgt.2014.69.
- 794 de Souza, W. F., Fortunato-Miranda, N., Robbs, B. K., de Araujo, W. M., de-Freitas-  
795 Junior, J. C., Bastos, L. G., et al. (2013). Claudin-3 overexpression increases the

- 796 malignant potential of colorectal cancer cells: roles of ERK1/2 and PI3K-Akt as  
797 modulators of EGFR signaling. *PLoS One* 8, e74994.  
798 doi:10.1371/journal.pone.0074994.
- 799 Szulc, J., Wiznerowicz, M., Sauvain, M.-O., Trono, D., and Aebischer, P. (2006). A  
800 versatile tool for conditional gene expression and knockdown. *Nat. Methods* 3, 109–  
801 116. doi:10.1038/nmeth846.
- 802 Vargas, J. E., Salton, G., Sodr  de Castro Laino, A., Pires, T. D., Bonamino, M., Lenz,  
803 G., et al. (2012). pLR: a lentiviral backbone series to stable transduction of  
804 bicistronic genes and exchange of promoters. *Plasmid* 68, 179–185.  
805 doi:10.1016/j.plasmid.2012.06.001.
- 806 Wang, T., Upponi, J. R., and Torchilin, V. P. (2012). Design of multifunctional non-viral  
807 gene vectors to overcome physiological barriers: dilemmas and strategies. *Int. J.*  
808 *Pharm.* 427, 3–20. doi:10.1016/j.ijpharm.2011.07.013.
- 809 Weber, K., Bartsch, U., Stocking, C., and Fehse, B. (2008). A Multicolor Panel of Novel  
810 Lentiviral “Gene Ontology” (LeGO) Vectors for Functional Gene Analysis. *Mol.*  
811 *Ther.* 16, 698–706. doi:10.1038/mt.2008.6.
- 812 Yarmush, M. L., Golberg, A., Serša, G., Kotnik, T., and Miklavčič, D. (2014).  
813 Electroporation-based technologies for medicine: principles, applications, and  
814 challenges. *Annu. Rev. Biomed. Eng.* 16, 295–320. doi:10.1146/annurev-bioeng-  
815 071813-104622.
- 816 Yin, H., Kanasty, R. L., Eltoukhy, A. A., Vegas, A. J., Dorkin, J. R., and Anderson, D.  
817 G. (2014). Non-viral vectors for gene-based therapy. *Nat. Rev. Genet.* 15, 541–555.  
818 doi:10.1038/nrg3763.
- 819